Research

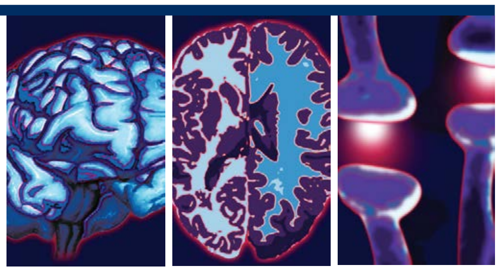

Increased Levels of Reactive Oxygen Species in Brain Slices after Transient Hypoxia Induced By a Reduced Oxygen Supply

Toru Sasaki†, Takuji Awaji, Kazuyoshi Shimada, Haruyo Sasaki

ABSTRACT

Background: Reactive oxygen species (ROS) have been suggested to be involved in cellular damage caused by ischemia-reperfusion, anoxia-reperfusion, and hypoxia-reperfusion. We previously demonstrated that the generation of ROS was enhanced following hypoxia caused by an increased oxygen demand, and this was related to a shift in the tissue redox balance toward reduction. The aim of the present study was to elucidate the relationship among changes in ROS generation, tissue pO_2 levels, and redox balance changes in brain slices following hypoxia caused by a decreased oxygen supply.

Methods

We measured ROS-dependent chemiluminescence in cerebral cortex slices using a photonic imaging method as well as tissue pO_2 levels and the redox balance using micro sensors during reoxygenation after hypoxia caused by the deprivation of an adequate oxygen supply.

Results

ROS-dependent chemiluminescent intensity was transiently enhanced during reoxygenation after the hypoxic treatment. Tissue pO_2 levels decreased and the tissue redox balance shifted towards reduction with the hypoxic treatment, followed by restoration to the steady-state condition. Increased ROS generation following hypoxia was related to a transient decrease in tissue pO_2 levels and a shift in the tissue redox balance towards reduction.

Conclusions

The present results demonstrated that ROS generation increased following hypoxia caused by a decreased oxygen supply. In addition, a transient redox shift to "hyper-reduction" with pO_2 changes may be involved in ROS generation in tissue.

Keywords

Reactive oxygen species, Hypoxia-reoxygenation, Brain slice, Redox, Hyper-reduction

Introduction

Reactive oxygen species (ROS) are considered to play a significant role in injury responses to ischemia and reperfusion as well as hypoxia and reoxygenation [1-3]. ROS generation increases during reoxygenation after hypoxia caused by a decreased oxygen supply. The status, in which oxygen consumption is enhanced beyond its supply, is regarded as another type of hypoxia. A decrease in tissue oxygen partial pressure

Department of Medical Engineering and Technology, Kitasato University School of Allied of Health Sciences, Japan

†Author for correspondence: Toru Sasaki, Department of Medical Engineering and Technology, Kitasato University School of Allied of Health Sciences, 1-15-1 Kitasato, Sagamihara, Kanagawa 252-0373, Japan, Tel: +81 42 778 8157; Fax: +81 42 778 9628; email: tsasaki@kitasato-u.ac.jp

(pO_2) has been reported in a seizure-like animal model [4,5]. However, it currently remains unclear whether ROS generation in the brain also increases during the restoration of hypoxia caused by a greater oxygen demand.

Ex-vivo brain slices have been used as a well-known model for electro-physiological studies in animal brain for half century [6]. Such measurements are performed in brain slices being a kind of steady state, which is keeping a living ability. This steady state is usually kept for several hours. In these experiments, slices were submersed with oxygenated 95%O_2/5%CO_2 media, because tissue pO_2 steeply decreased from the surface to tissue core [7-9]. Therefore, the oxygen concentration 95%O_2/5%CO_2 may be hyperoxic condition at slice surface cells whereas it may be hypoxic at the slice core. The thin-slicing has a merit to derive the sufficient oxygen into the mid of the slice, however it cannot be adopted for slice experiments because it causes neuronal damage by disrupting the long-range connections. The electrophysiological studies with direct measurements of slice tissue oxygenation indicated that a strong dependence of neuronal functions on oxygen in the range of pO_2 (10–400 Torr) [10-12] exceeded the physiological pO_2 range (10–60 Torr) in brain tissue *in vivo* [13,14]. These facts suggest that the oxygen concentration requirement for neuronal function is much higher in slices than in vivo.

We previously demonstrated that ROS-dependent chemiluminescence in the ex-vivo brain slices increased during the restoration of hypoxia caused by an enhanced oxygen demand using a novel photonic imaging method. Our findings suggested that ROS generation does not directly depend on the energy metabolic rate; it may be related to a transient decrease in tissue pO_2 levels and a shift in the tissue redox balance towards reduction. We also reported that ROS-dependent chemiluminescence in the brain increased during reoxygenation after hypoxia caused by the deprivation of an adequate oxygen supply [15-19]. However, the relationships among ROS generation, tissue pO_2 levels, and the redox balance during the restoration of hypoxia caused by a decreased oxygen supply have not yet been investigated. Therefore, we herein examined superoxide-dependent chemiluminescence in cerebral cortex slices as well as tissue pO_2 levels and the redox balance during reoxygenation after hypoxia caused by the deprivation of an oxygen supply.

Materials and Methods

■ Preparation of brain slices

Three-month-old male Wistar rats were purchased from Japan SLC Inc. (Shizuoka, Japan), and bred in the animal facility of Kitasato University School of Allied of Health Sciences. Animals were sacrificed by decapitation under anesthesia with an intraperitoneal injection of sodium pentobarbital (45 mg/kg body weight), and their brains were rapidly removed and placed on a tissue cutter (Microslicer DTK-3000W; Dosaka EM, Kyoto, Japan). Coronal slices cut at a thickness of 300 μm were transferred into ice-cold Krebs-Ringer solution (124 mM NaCl, 3 mM KCl, 2 mM $MgCl_2$, 1.3 mM NaH_2PO_4, 26 mM $NaHCO_3$, 10 mM glucose, and 200 mM sucrose) [20] equilibrated with 95% O_2/5% CO_2. Eight brain slices from each rat were pre-incubated at 34°C for 45 min in a chamber filled with 50 mL of 95% O_2/5% CO_2 gas-saturated Krebs-Ringer solution. The animal experimental protocol entitled "Elucidation of the molecular mechanism of reactive oxygen species generation using a molecular imaging technique" was approved by the Kitasato University School of Allied of Health Sciences Animal Care and Use Committee on 28 April, 2014. The approval number is 14-39. All procedures on animals were performed in accordance with the Kitasato University School of Allied of Health Sciences Guide for the Care and Use of Laboratory Animals.

■ System components

The apparatus comprised a culturing chamber, photon-counting camera (Intensified CCD camera C-2400-35; Hamamatsu Photonics K.K., Hamamatsu, Japan), imaging chamber (temperature-controlled dark box; Aloka Co. Ltd., Tokyo, Japan), and image controller (ARGUS-20; Hamamatsu Photonics K.K.), as previously reported [15]. Brain slices were arranged on a nylon net in the inner chamber and were lightly fixed in place by covering them with a fine net that was stretched and glued to the upper side of a 300-μm-thick stainless-steel ring. The field-of-view of image acquisition was 4 cm × 3 cm and contained 752 × 582 pixels.

Chemiluminescent image acquisition in cerebral cortex slices during normoxia, hypoxia, and reoxygenation.

The treatment of brain slices for the investigation of hypoxia-reoxygenation (30 min normoxia, 15 min hypoxia, and 120 min reoxygenation) was performed as described previously [21]. Briefly, after a 45-min preincubation period, slices were transferred into Krebs-Ringer solution (124 mM NaCl, 5 mM KCl, 2 mM $CaCl_2$, 1 mM $MgCl_2$, 1.2 mM KH_2PO_4, 26 mM $NaHCO_3$, and 10 mM glucose) containing 100 μM of N, N'-dimethyl-9, 9'-biacridinium dinitrate (lucigenin) equilibrated with 95% O_2/5% CO_2 for normoxic conditions and were incubated for additional 120 min in an imaging chamber at 34°C. They were then incubated under hypoxic (95% N_2/5% CO_2) conditions for 15 min before being returned to normoxic conditions for 120 min. Images of brain slices were acquired every 15 minutes during normoxia and hypoxia-reoxygenation for up to 255 min (11 frames). Images were acquired under a 9 cm × 12 cm field-of-view. A region of interest (ROI) was placed on the cerebral cortex. Chemiluminescent emission was expressed as "counts/pixel/min", which represented chemiluminescent emission per unit area in 15 min. The steady-state level of chemiluminescent emission under normoxia was expressed as "counts/pixel/min", which was calculated by averaging the chemiluminescent intensity of eight brain slices from each rat in the 30 minutes prior to the hypoxic treatment, while that of hypoxia-reoxygenation was calculated during the 45-minute post-hypoxic treatment. The experiment was performed using eight different animals, and the values of chemiluminescence emission (counts/pixel/min) under normoxic (90-120 min), hypoxic (120-135 min), and reoxygenic (150-195 min) conditions were averaged and expressed as the mean ± SD, as shown in **Figure 1**.

■ Measurement of tissue pO_2 levels and redox potential in cerebral cortex slices during normoxia, hypoxia, and reoxygenation

Brain slices (400-μm-thick) were prepared from male Wistar rats, as described above. After a 45-min preincubation period, slices were transferred into Krebs-Ringer solution equilibrated with 95% O_2/5% CO_2 in an imaging chamber at 34°C, as described above. A Clark type oxygen microelectrode (Ox-10; diameter 10 μ; Unisense, Aarhus, Denmark) was used to measure tissue pO_2 levels. The electrode was connected to a high-impedance millivoltmeter (Microsensor Multimeter; Unisense, Aarhus, Denmark). The electrode was calibrated by a two-point calibration using 100% oxygen-saturated (100%-point) and 100% nitrogen-saturated (0%-point) distilled water. A redox microelectrode (Ox-10; diameter 10 μm; Unisense, Aarhus, Denmark) and reference Ag/AgCl electrode (REF-321; diameter 8 mm; Unisense, Aarhus, Denmark) connected to a high-impedance millivoltmeter were used to measure tissue redox potential. The electrodes were calibrated by a two-point calibration using quinhydrone redox solutions (1% w/v of quinhydrone in pH 4 or pH 7 buffer solution (HORIBA, Ltd., Kyoto, Japan)). The electrode was positioned on the surface

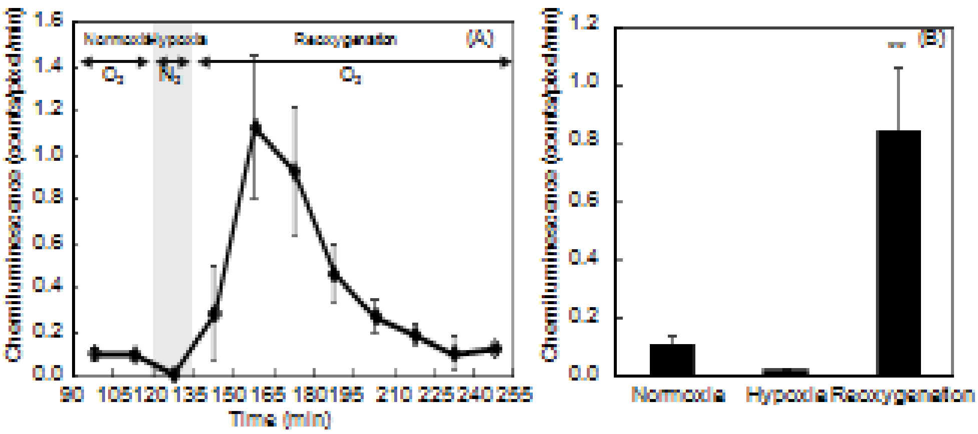

Figure 1: Time course of superoxide-dependent chemiluminescent intensity in the cerebral cortex during oxygenation and hypoxia-reoxygenation (A). Chemiluminescent images in cerebral cortex slices were acquired every 15 minutes under normoxic (90-120 min), hypoxic (120-135 min), and reoxygenic (135-255 min) conditions. Chemiluminescent intensity was expressed as "counts/pixel/min", which represents chemiluminescent emission per unit area in 15 min. The experiment was performed using eight different animals, and the value of chemiluminescent intensity was averaged and expressed as the mean ± SD. Comparison of averaged superoxide-dependent chemiluminescent intensities in cerebral cortex slices among normoxic (90-120 min), hypoxic (120-135 min), and reoxygenic (150-195 min) conditions (B). The experiment was performed using eight different animals, and the value of chemiluminescent emission (counts/pixel/min) was averaged and expressed as the mean ± SD. The significance of differences was analyzed using a one-way ANOVA with Scheffé's test ($p<0.01$** significantly different from normoxic and hypoxic levels).

of the cerebral cortex slice, and then lowered at 20-µm increments to a depth of 200 µm using a micromanipulator (Unisense, Aarhus, Denmark). pO_2 levels and the redox potential in the cerebral cortex slice were recorded every minute under normoxic (90-120 min), hypoxic (120-135 min), and reoxygenic (135-255 min) conditions.

The experiment was performed using four different animals, and the values of pO_2 (hPa) and redox potential (mV) in cerebral cortex slices at each time point were averaged and plotted in **Figures 2 and 3**. Mean pO_2 and redox potential levels under normoxic (90-120 min), hypoxic (120-135 min), and reoxygenic (150-195 min) conditions were averaged from four rats and expressed as the mean ± SD (**Figures 2 and 3**). The significance of differences was analyzed using a one-way ANOVA with Scheffé's test.

Results

■ Time course of superoxide-dependent chemiluminescent intensity in cerebral cortex slices during normoxia, hypoxia, and reoxygenation

The time course of superoxide-dependent chemiluminescent intensity in cerebral cortex slices collected from rats was shown in **Figure 1**. The steady-state level of chemiluminescent intensity under normoxic conditions was decreased by the hypoxic treatment, enhanced during reoxygenation, and then reached a maximum (10.5-fold the normoxic level) 30 min after the hypoxic treatment. Average chemiluminescent emission intensity in reoxygenation was 7.6-fold and 42.3-fold those in normoxia and hypoxia, respectively **(Figure 1)**.

Time course of pO_2 and redox potential levels in cerebral cortex slices during normoxia, hypoxia, and reoxygenation

The steady-state level of tissue pO_2 in the cerebral cortex was significantly decreased by the hypoxic treatment. Decreased pO_2 levels were then restored to normoxic levels **(Figure 2)**. The steady-state level of the tissue redox potential under normoxic conditions shifted to a more negative potential (from 252 mV to -87 mV). This redox balance shift towards reduction by the hypoxic treatment was restored to its normoxic level **(Figure 3)**.

Discussion

We previously demonstrated that ROS-dependent chemiluminescence in the brain increased during reoxygenation after hypoxia caused by the deprivation of an adequate oxygen supply using a photonic imaging method with lucigen, a chemilumigenic probe [15-19]. Due to its high sensitivity, lucigenin has been frequently used to detect superoxide anion radicals produced by enzymatic and cellular systems in tissue and isolated heart slices [20-26]. Lucigenin reacts not only with superoxide, yielding a product that emits chemiluminescence, but also with hydrogen peroxide under alkaline conditions. However, at physiological pH, lucigenin-derived

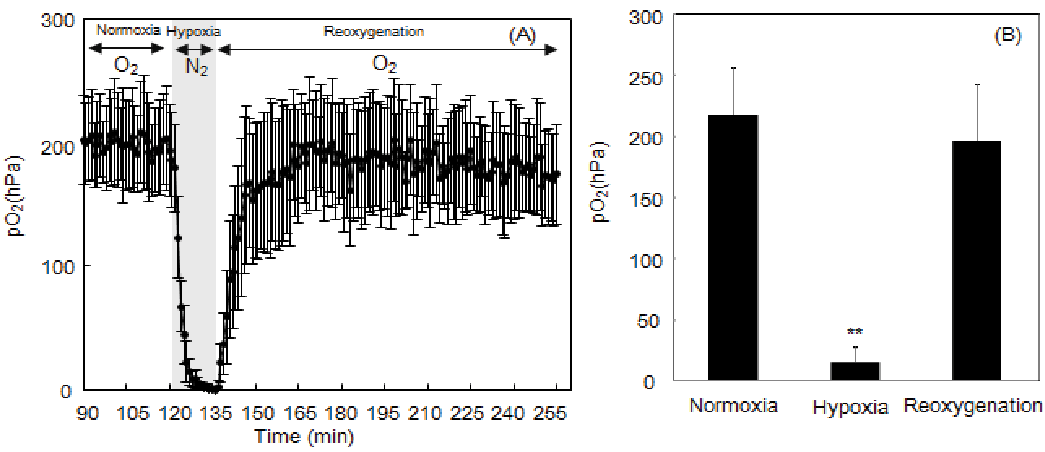

Figure 2: Time course of tissue oxygen partial pressure (pO_2) in the cerebral cortex during oxygenation and hypoxia-reoxygenation (A). pO_2 was recorded in cerebral cortex slices every minute under normoxic (90-120 min), hypoxic (120-135 min), and reoxygenic (135-255 min) conditions. Mean pO_2 levels under normoxic (90-120 min), hypoxic (150-195 min), and reoxygenic (135-180 min) conditions were averaged from four rats and expressed as the mean ± SD (B). The significance of differences was analyzed using a one-way ANOVA with Scheffé's test (p<0.01** significantly different from the normoxic level).

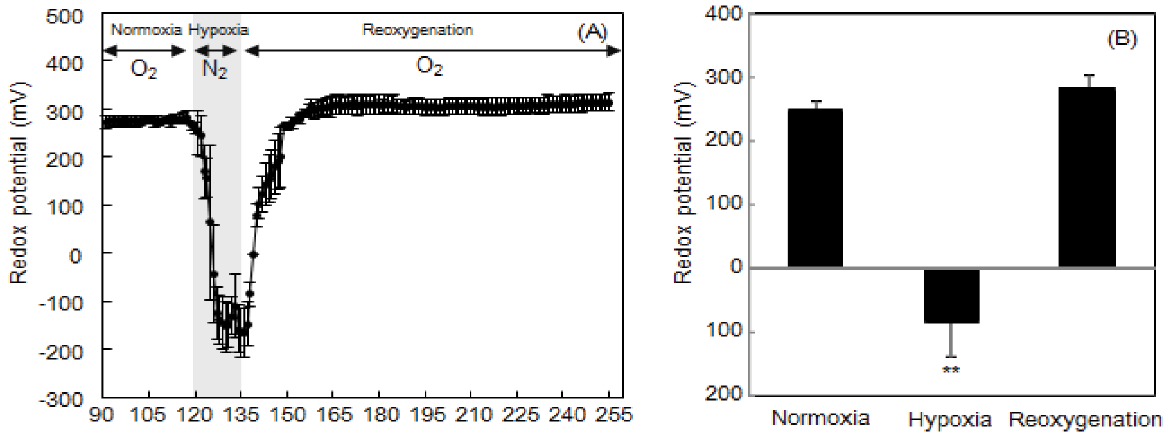

Figure 3: Time course of tissue redox potential (mV) in the cerebral cortex during oxygenation and hypoxia-reoxygenation (A). Redox potential was recorded in cerebral cortex slices every minute under normoxic (90-120 min), hypoxic (120-135 min), and reoxygenic (135-255 min) conditions. Mean redox potential levels under normoxic (90-120 min), hypoxic (120-135 min), and reoxygenic (150-195 min) conditions were averaged from four rats and expressed as the mean ± SD (B). The significance of differences was analyzed using a one-way ANOVA with Scheffé's test ($p<0.01$** significantly different from the normoxic level).

chemiluminescence represents superoxide levels in cells and tissues [27,28]. We indicated that lucigenin-derived chemiluminescence is derived from intracellular superoxide because lucigenin-derived chemiluminescence intensity was significantly decreased by EUK-8, a membrane-permeable superoxide dismutase (SOD)/catalase mimic, but not by Cu,Zn-SOD [17]. However, a major limitation of lucigenin is artifactual luminescence generation due to the production of superoxide by redox cycling with molecular oxygen, which may cause a high background [23,29].

Hypoxia is defined as a status in which tissue oxygen concentrations are insufficient to meet demands. Another type of hypoxia is conceivable as enhanced tissue oxygen consumption beyond its supply. Decreases in tissue pO_2 levels have been reported in a seizure-like animal model [4,5]. In *ex vivo* experiments, decreases in pO_2 levels, reflecting enhanced neural activity-dependent oxygen consumption, was demonstrated in electrical-, high potassium-, and odor stimulant-treated brain slices [10,30-34], while biphasic changes in tissue pO_2 responses, an initial decrease and subsequent increase due to enhanced cerebral blood flow, were found in activated brain regions in *in vivo* experiments [30,31]. We previously showed that ROS generation may be increased during the restoration of hypoxia caused by a greater oxygen demand [35]. In that study, ROS generation in tissue was enhanced after high potassium-induced hypoxia, and the high potassium treatment induced a transient decrease in tissue pO_2 levels as well as a shift in the tissue redox balance towards reduction. We herein investigated whether the tissue redox balance transiently shifted towards reduction due to a decreased oxygen supply and also if its recovery correlated with ROS generation. We also confirmed that superoxide-dependent chemiluminescence in cerebral cortex slices was transiently enhanced in response to tissue pO_2 levels and the redox balance **(Figure 1-3)**.

Mitochondria have been suggested as major sites for the intracellular generation of ROS, and the electrons that leak from the mitochondrial respiratory chain cause the partial reduction of molecular oxygen to the superoxide anion [36]. The intra-mitochondrion sites of ROS generation under the restoration process of transiently enhanced energy expenditure have been suggested to be complexes I and III. The blockage of the mitochondrial electron transfer chain enhances ROS generation from upstream of redox centers, whereas it minimizes ROS generation from downstream of these centers [37-41]. Previously, we analyzed lucigenine-enhanced chemiluminescence emission in slices of brain tissue prepared from Mn-SOD (located in mitochondria) and Cu, Zn-SOD (located in cytoplasm)-deficient mice to estimate the superoxide levels in mitochondria and cytoplasm. The enhanced chemiluminescence with Mn-SOD and Cu,Zn-SOD deficiency indicated that superoxide level in mitochondria was lower than that in cytoplasm, however the superoxide concentration was assumed to be higher in mitochondrial than the cytoplasm [18]. We also demonstrated that complexes I, III, and IV of the mitochondrial electron transfer chain are major sites for the generation of superoxide during the reoxygenation of hypoxia induced by a decreased oxygen supply, because the chemiluminescence in brain tissues was transiently enhanced by complex I inhibition by rotenone, complex III inhibition by antimycin A, and complex IV inhibition by cyanide. The upstream electron-rich status could be responsible for transiently increased superoxide generation by mitochondrial electron transfer chain inhibition [17].

Electrical stimuli are known to decrease pO_2 levels due to the early oxidation of mitochondrial NADH, followed by a prolonged redox balance of the $NADH/NAD^+$ shift towards reduction [33,42] because increased energy generation requires more oxygen and NADH for mitochondrial oxidative phosphorylation. In hippocampal slices, the redox shift of mitochondrial $NADH/NAD^+$ towards reduction also occurs during anoxia, while hyperoxidation has been reported during postanoxia [43,44]. The reduced oxygen supply in brain slices inhibited NAD(P)H oxidation parallel to the decrease in neuronal activity [45]. In *in vivo* models of seizure and anoxia, the mitochondrial redox balance of $NADH/NAD^+$ was also found to shift towards reduction [46]. High succinate concentration accumulates under ischemia/hypoxia in various tissues. Upon reperfusion, the accumulated succinate is rapidly re-oxidized by succinate dehydrogenase, driving the ROS generation by reverse electron transport at mitochondria [47]. Recent report indicates that the transition of mitochondrial complex I in the dormant form (D-form) during ischemia to the active form (A-form) after ischemia at early stage of reperfusion plays a significant role in ROS generation. In ischemic tissue, most of the complex I is present in the D-form, it is the state that an over-reduction of the upstream redox centers. If oxygen introduced to the reduced form of complex I ROS generation site, that results in an apparent increase in the rate of superoxide generation rates at flavin site [48]. Increased superoxide and hydrogen peroxide generation from the complex I expected for time needed for slow D-form to A-form transformation and restoration of the normal ubiquinone reductase activity. The ROS-generation activity of complex I depends on the matrix redox potential ($NADH/NAD^+$). Indeed, the superoxide and hydrogen peroxide generation from the complex I increased with NADH concentration dependence [49].

The results of present and our previous [35] studies suggested that the redox balance shift towards reduction, namely, "hyper-reduction" in tissue may participate in increased superoxide generation under the restoration of transient hypoxia induced by a decreased oxygen supply and increased oxygen demand.

Conclusion

ROS-dependent chemiluminescent intensity was transiently enhanced during reoxygenation after hypoxia induced by a decreased oxygen supply. Increased ROS generation following hypoxia was related to a transient decrease in tissue pO_2 levels and a shift in the tissue redox balance towards reduction. We suggest that the redox balance shift towards reduction, namely, "hyper-reduction" in tissue and mitochondria may participate in increased superoxide generation under the restoration of transient hypoxia induced by a decreased oxygen supply and increased oxygen demand.

References

1. Li C, Jackson RM. Reactive species mechanisms of cellular hypoxia-reoxygenation injury. Am. J. Physiol. Cell. Physiol 282(2), C227-241 (2002).
2. Dhar-Mascareño M, Cárcamo JM, Golde DW. Hypoxia-reoxygenation-induced mitochondrial damage and apoptosis in human endothelial cells are inhibited by vitamin C. Free Radic. Biol. Med 38(10), 1311-1322 (2005).
3. Margaill I, Plotkine M, Lerouet D. Antioxidant strategies in the treatment of stroke. Free Radic. Biol. Med 39(4), 429-443.
4. Martin RM, Halsey JH Jr. Local PO_2 and unit activity measured with an oxygen microelectrode from the gerbil cerebral cortex during seizure and EEG suppression. Adv. Exp. Med. Biol 159(1), 175-180 (1983).
5. Zhang C, Bélanger S, Pouliot P, *et al.* Measurement of local partial pressure of oxygen in the brain tissue under normoxia and epilepsy with phosphorescence lifetime microscopy. PLoS. One 25 10(8), e0135536 (2015).
6. Collingridge GL. The brain slice preparation: a tribute to the pioneer Henry McIlwain. J. Neurosci. Methods 59(1), 5-9 (1995).
7. Mulkey DK, Henderson RA 3rd, Olson JE, *et al.* Oxygen measurements in brain stem slices exposed to normobaric hyperoxia and hyperbaric oxygen. J. Appl. Physiol 90(5), 1887-1899 (2001).
8. Ivanov A, Zilberter Y. Critical state of energy metabolism in brain slices: the principal role of oxygen delivery and energy substrates in shaping neuronal activity. Front. Neuroenergetics 29(1), 3:9 (2011).
9. Engl E, Jolivet R, Hall CN, *et al.* Non-signalling energy use in the developing rat brain. J. Cereb. Blood Flow Metab 37(3), 951-966 (2017).
10. Foster KA, Beaver CJ, Turner DA. Interaction between tissue oxygen tension and NADH imaging during synaptic stimulation and hypoxia in rat hippocampal slices. Neuroscience 132 (3), 645-657 (2005).
11. Ivanov A, Mukhtarov M, Bregestovski P, *et al.* Lactate effectively covers energy demands during neuronal network activity

in neonatal hippocampal slices. Front. Neuroenergetics 6(1), 3-2 (2011).

12. Kann O, Huchzermeyer C, Kovács R, *et al.* Gamma oscillations in the hippocampus require high complex I gene expression and strong functional performance of mitochondria. Brain 134(Pt 2), 345-358 (2011).

13. Masamoto K, Kurachi T, Takizawa N, *et al.* Successive depth variations in microvascular distribution of rat somatosensory cortex. Brain. Res 995(1), 66-75 (2004).

14. Takano T, Tian GF, Peng W, *et al.* Cortical spreading depression causes and coincides with tissue hypoxia. Nat. Neurosci 10(6), 754-762 (2007).

15. Sasaki T, Iwamoto A, Tsuboi H, *et al.* Development of real-time bioradiographic system for functional and metabolic imaging in living brain tissue. Brain. Res 1077 (1), 161-169 (2006).

16. Sasaki T, Nariai T, Maehara T, *et al.* A comparative study of bioradiography in human brain slices and preoperative PET imaging. Brain. Res 1142(1), 19-27 (2007).

17. Sasaki T, Unno K, Tahara S, *et al.* Age-related increase of superoxide generation in the brains of mammals and birds. Aging. Cell 7(4), 459-469 (2008).

18. Sasaki T, Shimizu T, Koyama T, *et al.* Superoxide dismutase deficiency enhances superoxide levels in brain tissues during oxygenation and hypoxia-reoxygenation. J. Neurosci. Res 89 (4), 601-610 (2011).

19. Sasaki T, Yamanaka M, Kagami N. Superoxide generation in different brain regions of rats during normoxia and hypoxia-reoxygenation. Neurosci. Res 74 (3-4), 261-268 (2012).

20. Richerson GB, Messer C. Effect of composition of experimental solutions on neuronal survival during rat brain slicing. Exp. Neurol 131 (1), 133-143 (1995).

21. Riepe MW, Kasischke, K, Raupach, A. Acetylsalicylic acid increases tolerance against hypoxic and chemical hypoxia. Stroke 28(10), 2006-2011 (1997).

22. Murphy ME, Sies H. Visible-range low-level chemiluminescence in biological systems. Methods Enzymol 186(1), 595-610 (1990).

23. Laurindo FR, de Souza HP, Pedro Mde A, *et al.* Redox aspects of vascular response to injury. Methods Enzymol 352(1), 432-454 (2002).

24. Dirnagl U, Lindauer U, Them A, *et al.* Global cerebral ischemia in the rat: online monitoring of oxygen free radical production using chemiluminescence in vivo. J. Cereb. Blood Flow Metab 15 (6), 929-940 (1995).

25. Schreiber SJ, Megow D, Raupach A, *et al.* Age-related changes of oxygen free radical production in the rat brain slice after hypoxia: on-line measurement using enhanced chemiluminescence. Brain Res 703 (1-2), 227-230 (1995).

26. Näpänkangas JP, Liimatta EV, Joensuu P, *et al.* Superoxide production during ischemia-reperfusion in the perfused rat heart: a comparison of two methods of measurement. J. Mol. Cell Cardiol 53 (6), 906-915 (2012).

27. Vanfleteren JR, De Vreese A. Rate of aerobic metabolism and superoxide production rate potential in the nematode Caenorhabditis elegans. J. Exp. Zool 274 (2), 93-100 (1996).

28. Li Y, Zhu H, Kuppusamy P, *et al.* Validation of lucigenin (bis-N-methylacridinium) as a chemilumigenic probe for detecting superoxide anion radical production by enzymatic and cellular systems. J. Biol. Chem 273 (4), 2015-2023 (1998).

29. Schepetkin IA. Lucigenin as a substrate of microsomal NAD(P)H-oxidoreductases. Biochemistry (Mosc) 64 (1), 25-32 (1999).

30. Masamoto K, Omura T, Takizawa N, *et al.* Biphasic changes in tissue partial pressure of oxygen closely related to localized neural activity in guinea pig auditory cortex. J. Cereb. Blood Flow Metab 23 (9), 1075-1084 (2003).

31. Offenhauser N, Thomsen K, Caesar K, *et al.* Activity-induced tissue oxygenation changes in rat cerebellar cortex: interplay of postsynaptic activation and blood flow. J. Physiol 565(Pt 1), 279-294 (2005).

32. Foster KA, Beaver CJ, Turner DA. Interaction between tissue oxygen tension and NADH imaging during synaptic stimulation and hypoxia in rat hippocampal slices. Neuroscience 132(3), 645-657 (2005)

33. Galeffi F, Somjen GG, Foster KA, *et al.* Simultaneous monitoring of tissue PO_2 and NADH fluorescence during synaptic stimulation and spreading depression reveals a transient dissociation between oxygen utilization and mitochondrial redox state in rat hippocampal slices. J. Cereb. Blood Flow Metab 31 (2), 626-639 (2011).

34. Kann O, Hollnagel JO, Elzoheiry S, *et al.* Energy and potassium ion homeostasis during gamma oscillations. Front. Mol. Neurosci 16(1), 9-47 (2016).

35. Sasaki T, Awaji T, Shimada K, *et al.* Increase of reactive oxygen species generation in cerebral cortex slices after the transiently enhanced metabolic activity. Neurosci. Res 123(1), 55-64 (2017).

36. Sanz A. Mitochondrial reactive oxygen species: Do they extend or shorten animal lifespan? Biochim. Biophys. Acta 1857(8), 1116-1126 (2016).

37. Herrero A, Barja G. 8-oxo-deoxyguanosine levels in heart and brain mitochondrial and nuclear DNA of two mammals and three birds in relation to their different rates of aging. Aging (Milano) 11(5), 294-300 (1999).

38. Sun J, Trumpower BL. Superoxide anion generation by the cytochrome bc1 complex. Arch. Biochem. Biophys 419(2), 198-206 (2003).

39. Chen Q, Vazquez EJ, Moghaddas S, *et al.* Production of reactive oxygen species by mitochondria: central role of complex III. J. Biol. Chem 278(38), 36027-36031 (2003).

40. Kudin AP, Bimpong-Buta NY, Vielhaber S, *et al.* Characterization of superoxide-producing sites in isolated brain mitochondria. J. Biol. Chem 279(6), 4127-4135 (2004).

41. Adam-Vizi V. Production of reactive oxygen species in brain mitochondria: contribution by electron transport chain and non-electron transport chain sources. Antioxid. Redox Signal 7(9-10), 1140-1149 (2005).

42. Galeffi F, Foster KA, Sadgrove MP, *et al.* Lactate uptake contributes to the NAD(P)H biphasic response and tissue oxygen response during synaptic stimulation in area CA1 of rat hippocampal slices. J. Neurochem 103(6), 2449-2461 (2007).

43. Perez-Pinzon MA, Mumford PL, Carranza V, *et al.* Calcium influx from the extracellular space promotes NADH hyperoxidation and electrical dysfunction after anoxia in hippocampal slices. J. Cereb. Blood Flow. Metab 18(2), 215-221 (1998).

44. Perez-Pinzon MA, Mumford PL, Rosenthal M, *et al.* Antioxidants, mitochondrial hyperoxidation and electrical recovery after anoxia in hippocampal slices. Brain Res 754(1-2), 163-170 (1997).

45. Ivanov A, Zilberter Y. Critical state of energy metabolism in brain slices: the principal role of oxygen delivery and energy substrates in shaping neuronal activity. Front. Neuroenergetics 29(1), 3-9 (2011).

46. Merrill DK, Guynn RW. The calculation of the mitochondrial free [NAD^+]/[NADH][H^+] ratio in brain: effect of electroconvulsive seizure. Brain. Res 239(1), 71-80 (1982).

47. Chouchani ET, Pell VR, Gaude E, *et al.* Ischaemic accumulation of succinate controls reperfusion injury through mitochondrial ROS. Nature 515(7527), 431-435 (2014).

48. Dröse S, Stepanova A, Galkin A. Ischemic A/D transition of mitochondrial complex I and its role in ROS generation. Biochim. Biophys. Acta 1857(7), 946-957 (2016).

49. Vinogradov AD, Grivennikova VG. Oxidation of NADH and ROS production by respiratory complex I. Biochim. Biophys. Acta 1857(7), 863-871 (2016).